

1 **Technical Note: Stability of tris pH buffer in artificial seawater**
2 **stored in bags**

3 Wiley H. Wolfe¹, Kenisha M. Shipley¹, Philip J. Bresnahan², Yuichiro Takeshita³, Taylor Wirth¹,
4 Todd R. Martz¹

5 ¹Scripps Institution of Oceanography, University of California San Diego, La Jolla, 92093, USA

6 ²Department of Earth and Ocean Sciences, University of North Carolina Wilmington, Wilmington, 28403, USA

7 ³Monterey Bay Aquarium Research Institute, Moss Landing, 95093, USA

8 *Correspondence To:* Philip J. Bresnahan Jr. (bresnahanp@uncw.edu)

9

10 **Abstract**

11 Equimolar tris (2-amino-2-hydroxymethyl-propane-1,3-diol) buffer in artificial seawater is a well characterized
12 and commonly used standard for oceanographic pH measurements. We evaluated the stability of tris pH when stored
13 in purportedly gas impermeable bags across a variety of experimental conditions, including bag type, and storage in
14 air vs. seawater over 300 days. Bench-top spectrophotometric pH analysis revealed that the pH of tris stored in bags
15 decreased at a rate of $0.0058 \pm 0.0011 \text{ yr}^{-1}$ (mean slope \pm 95% confidence interval of slope). Analyses of total dissolved
16 inorganic carbon confirmed that a combination of CO₂ infiltration and/or microbial respiration led to the observed
17 decrease in pH. Eliminating the change in pH of bagged tris remains a goal, yet the rate of pH change is lower than
18 many processes of interest and demonstrates the potential of bagged tris for sensor calibration and validation of
19 autonomous in situ pH measurements.

20 **1. Introduction**

21 Ocean pH is a key measurement used for tracking biogeochemical processes such as photosynthesis,
22 respiration, and calcification (Takeshita et al., 2016); and represents perhaps the most recognized variable associated
23 with ocean acidification (OA), the decrease in ocean pH due to the uptake of anthropogenic carbon dioxide (Doney et
24 al., 2009). OA progresses with a global average pH decline of 0.002 per year in the surface open ocean (Bates et al.,
25 2014), and the accumulated and projected near-term effects of OA have been shown to have deleterious effects on
26 many calcifying organisms (Cooley and Doney, 2009). Beyond the narrow scope of calcifiers, organismal response is
27 complex, exhibiting varied responses across processes such as reproduction, growth rate, and sensory perception.
28 Organismal responses are further complicated by their impact on ecosystem level dynamics, such as altering
29 competition and predator-prey relationships (Doney et al., 2020). Furthermore, pH effects are often exacerbated by
30 concomitant stressors, such as decreased dissolved oxygen or increased temperature. Ultimately, OA will affect
31 humans through impacts on fisheries, aquaculture, and shoreline protection (Branch et al., 2013; Doney et al., 2020).

32 The quality of pH measurement required to observe various phenomena is often broken into “climate” and
33 “weather” levels of uncertainty (Newton et al., 2015), or 0.003 and 0.02, respectively. Discrete sampling has been
34 shown to be capable of meeting the climate level of uncertainty when best practices are followed, yet many labs do
35 not consistently meet this standard (Bockmon and Dickson, 2015). Furthermore, while discrete, bench-top
36 methodologies can be the most accurate, the ocean’s vast size limits the oceanographic community’s ability to make
37 ship-based discrete pH measurements to decadal reoccupations of a few major sections per ocean basin (Sloyan et al.,
38 2019). The sparsity of ship-board measurements hinders our ability to assess sub-decadal processes, such as seasonal
39 cycles or bloom events, over much of the ocean (Karl, 2010), and highlights the need for autonomous, high-frequency
40 pH measurements. Technological advancements have led to more routine autonomous pH measurements over the past
41 decade, providing opportunities to fill some gaps in time and space in discrete sampling programs (e.g. Byrne, 2014;
42 Martz et al., 2015; Lai et al., 2018; Wang et al., 2019; Tilbrook et al., 2019). Globally, pH sensors now operate on
43 hundreds of autonomous platforms including moorings and profiling floats, delivering unique datasets in the form of
44 Eulerian and depth resolved Lagrangian time series (Johnson et al., 2017; Bushinsky et al., 2019; Sutton et al., 2019).

45 While sensors increase data coverage, many sensor-based pH measurements, particularly on moored systems, continue
46 to fall short of both climate and weather levels of uncertainty, as highlighted in the intercomparison tests carried out
47 by the Alliance for Coastal Technologies (ACT, 2012) and by the Wendy Schmidt Ocean Health XPRIZE (Okazaki
48 et al., 2017).

49 Independent validation is typically required for autonomous sensors to meet both weather and climate levels
50 of uncertainty. For example, autonomous underway $p\text{CO}_2$ systems (Pierrot et al., 2009), moorings (Bushinsky et al.,
51 2019), and autonomous surface vehicles (Chavez et al., 2017; Sabine et al., 2020) are able to provide climate quality
52 observations with an uncertainty of $\pm 2 \mu\text{atm}$ because traceable standard gases are frequently measured in situ. For pH
53 measurements on profiling floats (Johnson et al., 2016), sensor performance is validated by comparing to a deep
54 reference pH field that is calculated using empirical algorithms (Williams et al., 2016; Bittig et al., 2018; Carter et al.,
55 2018). This approach has demonstrated the ability to obtain high quality pH measurements from a network of profiling
56 floats (Johnson et al., 2017) but requires measurements in the deep ocean where pH is comparatively stable. It is
57 atypical for other pH sensors, including coastal moored sensors, to have an automated or remote validation. Therefore,
58 on such deployments, validation has largely relied on discrete samples taken alongside the sensor (Bresnahan et al.,
59 2014; McLaughlin et al., 2017; Takeshita et al., 2018), which presents unique challenges; primarily that spatiotemporal
60 discrepancy can lead to errors of > 0.1 , especially in highly dynamic systems (Bresnahan et al., 2014).

61 Similar to the method in use by $p\text{CO}_2$ systems, one approach to validate in situ pH sensors is by measuring a
62 reference material or pH standard, repeatedly during a sensor deployment. The most commonly used standard for
63 oceanographic pH measurement is equimolar tris (2-amino-2-hydroxymethyl-propane-1,3-diol) buffer in artificial
64 seawater (ASW), hereafter referred to as tris or tris-ASW (DeValls and Dickson, 1998; Papadimitriou et al., 2016).
65 The pH of tris has been characterized over a range of temperature, salinity, and pressure (DeValls and Dickson, 1998;
66 Rodriguez et al., 2015; Takeshita et al., 2017; Müller et al., 2018), allowing for accurate calculation of tris pH across
67 a wide range of marine conditions. Furthermore, when stored in borosilicate bottles and under ideal conditions, these
68 buffers have been shown to be stable to better than 0.0005 over a year (Dickson, 1993; Nemzer and Dickson, 2005),
69 making tris a good candidate for in situ validation of long term deployments of autonomous pH sensors. To be utilized
70 for in situ applications, the reference solution must be stored in bags (as in, Hales et al., 2005; Seidel et al., 2008;
71 Sayles and Eck, 2009; Spaulding et al., 2014; Wang et al., 2015; Lai et al., 2018). Recently, in situ sensor validation
72 using bagged tris was demonstrated by Lai et al. (2018) during a 150-day deployment of an autonomous pH sensor,
73 where the tris standard was measured in situ every 5 days. However, the stability of tris when stored in bags has not
74 been quantified systematically using spectrophotometric bench-top pH measurement techniques recommended as best
75 practices (Dickson et al., 2007).

76 In this work we quantified the stability of tris stored in bags for 300 days. Tris from four separately prepared
77 batches was stored in two bag types either in a lab or submerged in seawater. In addition, one batch was stored in
78 borosilicate bottles in the lab as a control. Spectrophotometric pH measurements were made approximately every two
79 months on each bag of tris. Throughout the experiment, Certified Reference Materials (CRMs) for oceanic CO_2
80 measurements (Dickson, 2001) were used to assess the stability of the spectrophotometric pH system.

81 2. Methods

82 Two bag types were tested for storing tris (Figure 1). Bag type 1 was custom made based on a design used in
83 the “Burke-o-Lator” system (Hales et al., 2005; Bandstra et al., 2006), made from PAKDRY 7500 barrier film
84 (IMPAK P75C0919). The barrier film is made of layers of polyester and nylon with a sealant layer of metallocene
85 polyethylene. Two 23 x 48 cm (9” x 19”) sheets were heat sealed on three sides, forming a pocket, and a 1.9 cm (3/4”)
86 diameter hole was cut into one of the pocket walls for the bulkhead fitting and bulkhead nut (McMaster-Carr
87 8674T55). The bulkhead was sealed into the wall with a silicone gasket (McMaster-Carr 9010K13), washer
88 (McMaster-Carr 95649A256), and coated with silicone sealant (McMaster-Carr 74955A53). A “push-to-connect” ball
89 valve fitting (McMaster-Carr 4379K41), was attached to the bulkhead. The modified pocket was rinsed, dried, and
90 heat sealed along the final edge to create a ~4 L bag. Bags were left to dry for at least 24 hours before filling. Bag type
91 2 was a commercially available 3 L Cali-5-Bond bag purchased from Calibrated Instruments and used without
92 modification. It is a multi-layer bag made of plastic, aluminium foil (to prevent liquid and gas permeation), a layer of
93 inert high density polyethylene (to form a non-reactive inner wall) and, a polycarbonate Stopcock Luer valve.

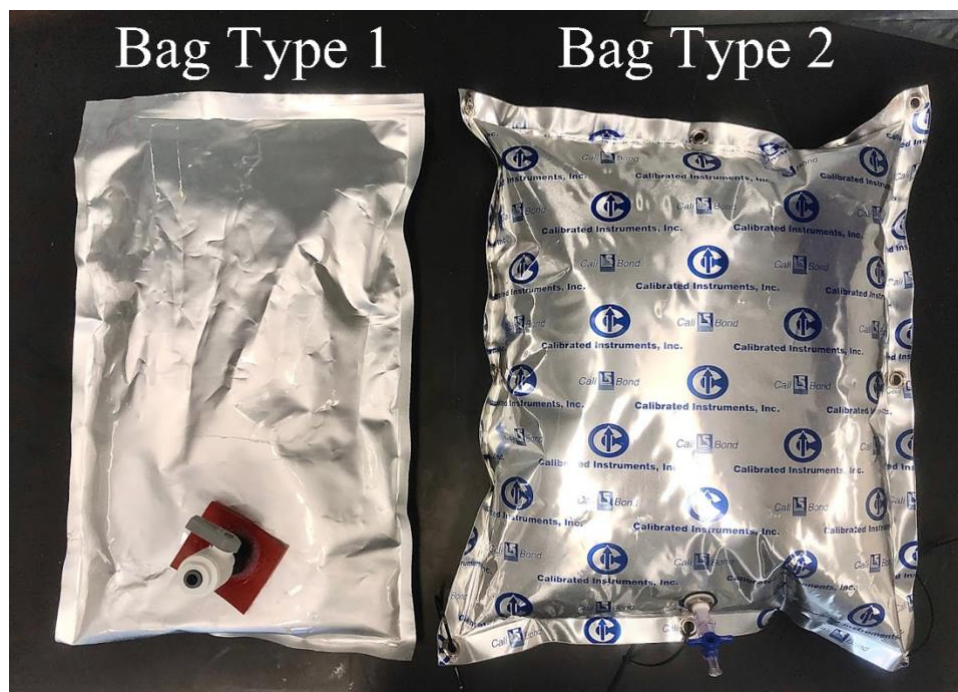


Figure 1: A picture of bag type 1 and 2 used to store tris in this study.

94 In this experiment, four batches of tris were prepared following the procedure in DelValls and Dickson
95 (1998), using off-the-shelf reagents with no additional standardization or purification (e.g. recrystallization of salts).
96 The focus of this paper is stability of bagged tris over time and does not prioritize obtaining highly accurate equimolar
97 tris (as would be necessary for characterization of thermodynamic constants, for example). The calculated pH of tris
98 in this study was 8.2652 at 20°C, based on quantity of reagents used. This is 0.0135 higher than the pH of equimolar
99 tris, 8.2517 at 20°C (DelValls and Dickson, 1998). The pH discrepancy was due to a unit error in the measurement of
100 HCl (our preparation used mol/L rather than the prescribed mol/kg-sol). This unit error resulted in a tris:trisH⁺
101 1:0.97 that slightly differs from the 1:1 of truly equimolar tris. As this ratio is nearly equimolar, the term “equimolar”

102 will continue to be used throughout this study. The details of the specific reagents used to prepare the tris solution can
 103 be found in Table A1.

104 Three stability tests were initiated at different times over the course of 18 months. The initiation of a given
 105 test is defined as the date of preparation of the tris used in that test. A summary of the differences between these tests
 106 is shown in Table 1 and described here. Each bag has a unique identifier in the format of “Batch #, Bag #, Lab or
 107 Tank.” If this identifier is duplicative, the bags are differentiated with letters A to D. Each bag was rinsed before
 108 filling: 3 times with deionized water (DI), 5 times with ultrapure water ($> 18 \text{ M}\Omega$ resistivity) and at least 3 times with
 109 200 mL of tris. Tris bags were stored on a lab bench or in a 5,000 L test tank filled with ozone-sterilized, filtered
 110 seawater. Bag type 2 experienced delamination of exterior layers when stored in seawater during test 2 and was not
 111 used in further testing. Tris from batch 4 was also stored in borosilicate bottles following the procedure in Nemzer
 112 and Dickson (2005). In addition to pH measurements, dissolved inorganic carbon (C_T) was measured on both bagged
 113 and bottled tris during test 3 to see if changes in pH were due to increased CO_2 . C_T samples were measured using a
 114 custom-built system based on an infrared (IR) analyser (LI-COR 7000) similar to systems used by O’Sullivan and
 115 Millero (1998) and Friederich et al. (2002). This IR measurement system is capable of measuring relatively low C_T
 116 without requiring method adjustment and has been used to make near zero C_T measurements (Paulsen and Dickson,
 117 unpublished data). C_T measurements were made on CRMs (Batch 179 & 183). The precision of the C_T measurements
 118 was $\pm 1.4 \mu\text{mol/kg}$ (pooled standard deviation, $n_{\text{samples}}=15$, $n_{\text{measurements}}=44$).

119 **Table 1: Tris preparation and storage.**

| | Bag Type | Tris Batch | Date Made | Storage Location | Rinse Procedure | C_T Measured |
|--------|------------|------------|------------------|------------------|--|----------------|
| Test 1 | 1 & 2 | 1 & 2 | 13 Dec 2017 | Lab & Tank | 3x DI, 5x ultrapure, 3x tris | No |
| Test 2 | 1 & 2 | 3 | 13 April 2018 | Lab & Tank | 3x DI, 5x ultrapure, 3x tris | No |
| Test 3 | 1 & bottle | 4 | 26 February 2019 | Lab | 3x DI, 5x ultrapure, $\geq 6x$ tris | Yes |

120
 121 Tris pH was measured every 55 ± 20 days (mean \pm standard deviation of measurement interval) throughout
 122 the experiment. The pH of tris was measured in triplicate at each time point with spectrophotometry using m-cresol
 123 purple as the indicator dye using the system described in Carter et al. (2013). Absorbance measurements were made
 124 in a 10-cm jacketed cell, and the temperature was measured directly adjacent to the cell outflow using a NIST-traceable
 125 thermometer ($\pm 0.1 \text{ }^\circ\text{C}$, QTI DTU6028P-001-SC). Blank and sample were held for 3 minutes in the jacketed flow cell
 126 prior to absorbance measurements.

127 On average, temperature was stable to within a $0.02 \text{ }^\circ\text{C}$ range over the course of the day; the mean temperature
 128 throughout the experiment was $20.09 \pm 0.23 \text{ }^\circ\text{C}$ (1σ), although temperature was $0.6 \text{ }^\circ\text{C}$ higher than the average on
 129 one measurement day. Spectrophotometric pH measurements are reported at $20 \text{ }^\circ\text{C}$ by adjusting the measured pH
 130 value at the measured cell temperature T_C (pH_{spec,T_C}) to $20 \text{ }^\circ\text{C}$ ($pH_{\text{spec},20^\circ\text{C}}$) using the known temperature dependence
 131 of tris (pH_{tris}) as follows:

$$pH_{spec,20^{\circ}C} = pH_{spec,T_C} - (pH_{tris,T_C} - pH_{tris,20^{\circ}C}) \quad (1)$$

132 pH_{tris,T_C} and $pH_{tris,20^{\circ}C}$ are the theoretical pH of tris (at the measured temperature and 20 °C respectively) and were
 133 calculated using Eq. (18) in DelValls and Dickson (1998). This adjustment assumes that any potential difference in
 134 $\partial pH/\partial T$ between that corresponding to equimolar tris and that corresponding to our 1:0.97 tris:trisH⁺ ratio has a
 135 negligible effect over the small temperature range observed.

136 To account for pH-dependent errors from impurities in unpurified mCP, a pH-dependent correction factor
 137 was determined based on the protocol outlined in Takeshita et al. (in review). Briefly, pH of seawater was measured
 138 subsequently using impure dye (pH_{impure} ; from Aldrich, lot MKBH6858V) and purified dye (pH_{pure} ; from Robert
 139 Byrne’s Lab, University of South Florida (Liu et al., 2011)) over a range of pH between 7.4 to 8.2 at approximately
 140 0.2 intervals. Varying ratios of tris:trisH⁺ were used to obtain different solution pH, and to buffer any changes in pH
 141 during the experiment, which negates the need for dye perturbation corrections in this characterization. Triplicate
 142 measurements were made at each pH. A second order pH-dependent error was observed as previously described,
 143 following the equation ($R^2 = 0.975$, RMSE = 0.000434):

$$pH_{pure} = -0.0047777 \times pH_{impure}^2 + 1.0668875 \times pH_{impure} - 0.2359740 \quad (2)$$

144 All subsequent pH_{spec} measurements in this study were conducted with impure dye and are reported with this dye
 145 impurity correction (Eq. 2) applied. The correction adjusted the reported pH by 0.0093 ± 0.0002 (mean \pm standard
 146 deviation, $n = 126$). No dye perturbation correction was used (a correction for a change in pH caused by the addition
 147 of the dye). As the high buffering capacity of tris, in combination with a dye adjusted to a pH similar to that of tris,
 148 results in a negligible change in measured pH.

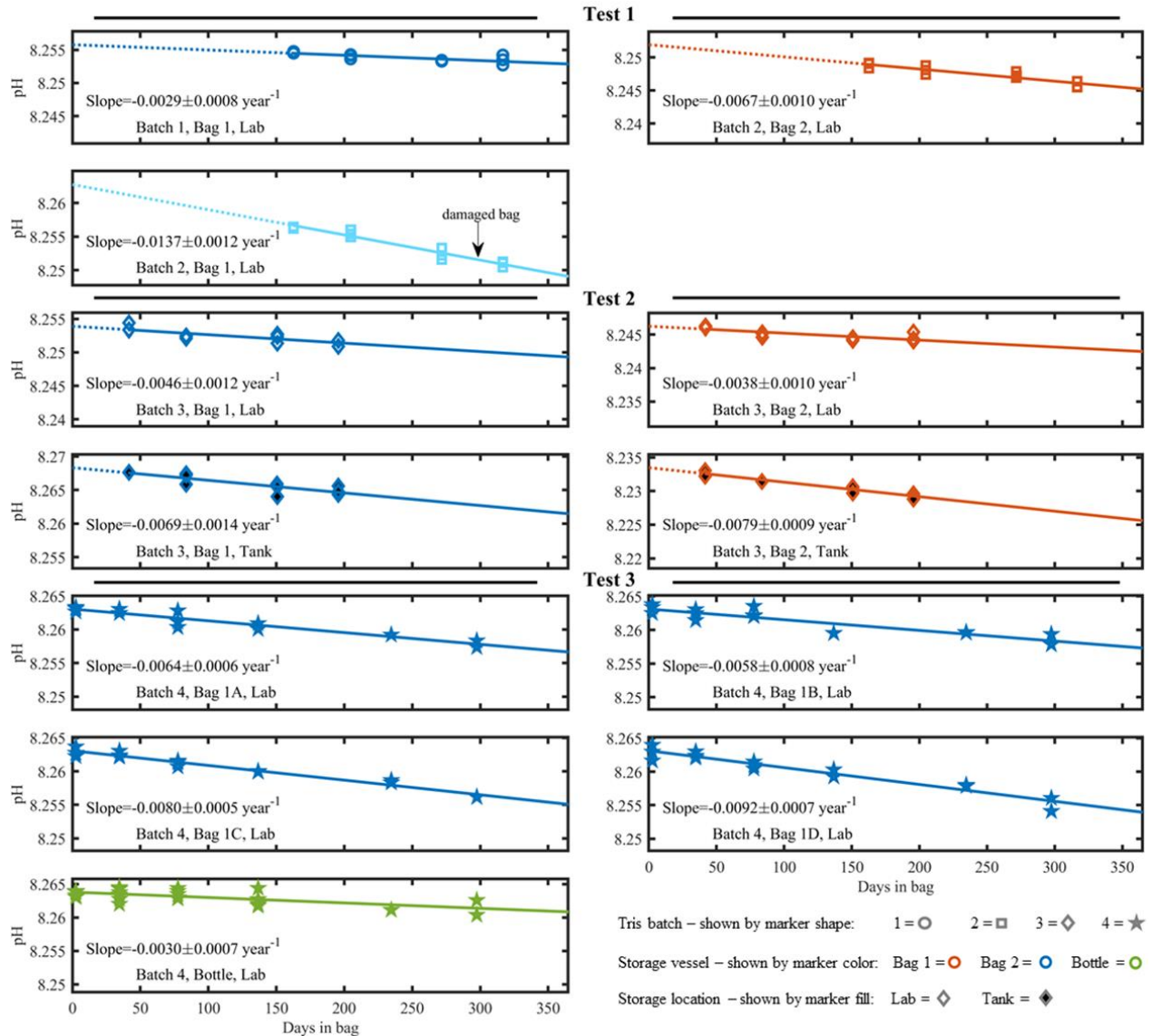
149 Measurements of tris batches 1 and 2 made in the first 150 days have been removed from the data set due to
 150 procedural changes made to the spectrophotometric pH system to correct for problems with temperature equilibration.
 151 Outliers were removed from the spectrophotometric pH measurements if the absorbance at 760 nm was above 0.005
 152 or below -0.002 (indicative of a measurement problem, such as a bubble or lamp drift), resulting in the removal of 2
 153 out of 163 measurements. Additionally, outliers were removed from the data set if they were greater than three
 154 standard deviations from the mean of a measurement triplicate, where standard deviation is calculated as using all sets
 155 of triplicates (1 standard deviation = 0.0004, $n = 55$), resulting in the removal of 2 of 161 remaining measurements.
 156 The remaining 159 measurements were used for the analysis presented here. An analysis of variation, or ANOVA,
 157 was used to detect the dependence of the results on tris batch, bag/bottle type and storage location. Analysis was
 158 performed using MATLAB R2020a and the standard function “`anovan()`.” Throughout the experiment, CRMs
 159 (procured from A. Dickson, Scripps Institution of Oceanography) for seawater C_T and total alkalinity were measured
 160 regularly to verify instrument performance (Dickson, 2001). A time-series of CRM measurements over the duration
 161 of the work described here showed no systematic drift. (Fig. A1 in Appendix A). To assess if the change in pH was
 162 driven by the addition of CO₂, the final pH and available C_T measurements were compared with a model described
 163 here. The theoretical change in tris-artificial seawater (ASW) pH due to an increase in C_T is straightforward to
 164 calculate, since both tris and CO₂ acid-base equilibria are well-characterized in seawater and ASW media. The pH is
 165 calculated for tris-ASW + C_T using an equilibrium model following the approach described in Chapter 2 of Dickson
 166 et al. (2007) for the case of known alkalinity and C_T . In the case of ASW, the seawater equilibrium constants for CO₂

167 are appropriate because minor ions present in seawater and not ASW do not appreciably affect the CO₂ equilibrium
168 constants (particularly when the goal is to compute relative changes in pH) as the ionic background of ASW is closely
169 matched to that of seawater at salinity = 35. In our model, minor acid-base species important to seawater alkalinity
170 but not present in ASW (borate, phosphate, silicate, fluoride) are set to zero. The definition of total alkalinity is
171 modified to include the tris acid-base system following the definition of acid-base donor/acceptor criteria given by
172 Dickson (1981): tris is assigned as a level-1 proton acceptor and tris-H⁺ is at the zero level. Thus, in our model, tris_{tot}
173 = 0.08 molal and alkalinity = 0.04 molal and C_T is a variable. An algorithm (see Annexe 1 in Dickson et al. (2007)) is
174 then used to find the root of the alkalinity equation in its residual form by solving for pH.

175 **3. Results & Discussion**

176 Figure 2 depicts pH_{spec,20°C}, stored in either a bag or bottle, as a function of time and is subdivided for tests 1,
177 2, and 3. A linear decrease was observed for all bags or bottles. A linear regression was calculated for each
178 experimental condition and, in the cases where measurements at t = 0 were removed due to protocol changes described
179 above, the line was extrapolated back to t = 0, shown by the dotted line. The measured or extrapolated y-intercept is
180 reported as the initial pH in Table 2. In all tests, trendlines are extrapolated to t = 365 days to illustrate observed and

181 predicted change over the course of a year as shown by the solid line. For ease of visual comparison, the y-axis of
 182 each subplot has an identical pH range of 0.017.
 183



184
 185 **Figure 2: Individual time series of measured pH in tris buffer solutions. Bag type 1 is shown in blue (light blue for the**
 186 **damaged bag of type 1), 2 in orange and bottle in green. Tris batch 1 is depicted as circles, 2 as squares, 3 as diamonds and**
 187 **4 as stars. Storage location in tank has a black fill and lab symbols have no fill. This marker system is also followed in Fig.**
 188 **A2. The solid line is a linear regression starting at the first included pH measurement and ending 365 days after the tris**
 189 **was bagged. The dotted line illustrates the extrapolation back to 0 days stored in bag when measurements at t = 0 do not**
 190 **exist. The range of the y-axis scale is fixed at 0.017 pH for all subplots.**

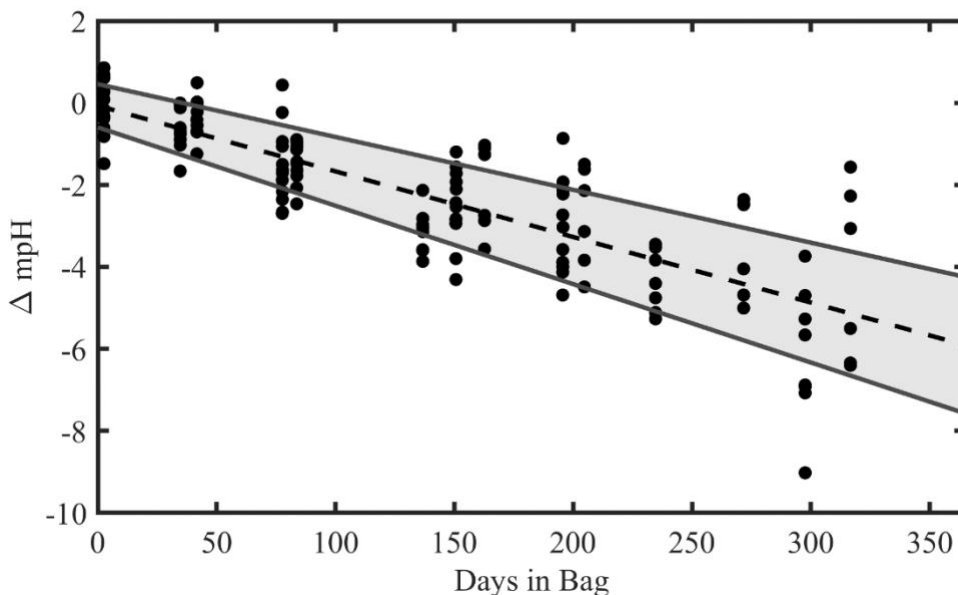
191

192 **Table 2: Linear regression statistics from trendlines shown in Fig. 1 and 2. The last row shows the regression statistics for**
 193 **tris from all batches, in either bag type, stored in the lab or test tank. Slope and intercept are shown as mean \pm 95%**
 194 **confidence intervals. The reported intercept is the regression intercept; when initial pH measurements are available, they**
 195 **differ by less than 0.0003 from regression intercept. * Indicates the outlier (Batch 2, Bag 1, Lab) caused by a damaged bag.**
 196 **The outlier, “Batch 2, Bag 1, lab”, was not used in the “All Batches, All Bags, Lab or Tank” composite. † In all batches, all**
 197 **bags, lab or tank, the slope was calculated with a linear fit of all (non-outlier) tris measurements. The RMSE is the mean**
 198 **RMSE of all (non-outlier) bag fits. ‡ The calculated tris pH was calculated at 20°C; however, this calculated pH is 0.0135**
 199 **higher than equimolar tris as noted above (DeValls and Dickson, 1998).**

| Batch & Storage Method | Slope (mpH yr ⁻¹) | Intercept (Initial pH) | RMSE (mpH) | r ² | n |
|-------------------------------------|-------------------------------|------------------------|------------|----------------|-----|
| Batch 1, Bag 1, Lab | -2.9 \pm 1.7 | 8.2558 \pm 0.0012 | 0.43 | 0.59 | 12 |
| Batch 2, Bag 1, Lab* | -13.7 \pm 2.7 | 8.2627 \pm 0.0018 | 0.61 | 0.94 | 11 |
| Batch 2, Bag 2, Lab | -6.7 \pm 2.2 | 8.2519 \pm 0.0015 | 0.55 | 0.82 | 12 |
| Batch 3, Bag 1, Lab | -4.6 \pm 2.7 | 8.2539 \pm 0.0010 | 0.62 | 0.62 | 11 |
| Batch 3, Bag 1, Tank | -6.9 \pm 3.2 | 8.2683 \pm 0.0012 | 0.73 | 0.73 | 11 |
| Batch 3, Bag 2, Lab | -3.8 \pm 2.1 | 8.2462 \pm 0.0008 | 0.54 | 0.61 | 12 |
| Batch 3, Bag 2, Tank | -7.9 \pm 2.1 | 8.2335 \pm 0.0008 | 0.44 | 0.92 | 9 |
| Batch 4, Bag 1A, Lab | -6.4 \pm 1.3 | 8.2630 \pm 0.0005 | 0.64 | 0.90 | 14 |
| Batch 4, Bag 1B, Lab | -5.8 \pm 1.8 | 8.2631 \pm 0.0008 | 0.91 | 0.79 | 15 |
| Batch 4, Bag 1C, Lab | -8.0 \pm 1.0 | 8.2631 \pm 0.0004 | 0.49 | 0.96 | 15 |
| Batch 4, Bag 1D, Lab | -9.2 \pm 1.6 | 8.2631 \pm 0.0007 | 0.80 | 0.92 | 15 |
| Batch 4, Bottle, Lab | -3.0 \pm 1.4 | 8.2638 \pm 0.0005 | 0.81 | 0.44 | 25 |
| All Batches, All Bags, Lab or Tank† | -5.8 \pm 1.1 | – | 0.72 | 0.66 | 126 |
| Calculated tris pH‡ | – | 8.2652 | – | – | – |

200
 201 Only bags from test 3, using tris batch 4 and bag type 1, have direct initial pH measurements and replicate
 202 bags. Initial pH measurements of these 4 bags were 8.2630 \pm 0.0007 (mean \pm standard deviation, n = 12). Importantly,
 203 the very low standard deviation suggests that a single initial pH measurement is representative of all replicate bags
 204 filled with a single tris batch, if the preparation procedure used in test 3 is followed. This inter-bag consistency is
 205 beneficial because it reduces the number of initial pH measurements required when filling multiple bags. There is also
 206 strong agreement in initial pH measurements between bagged and bottled tris in test 3, with the initial pH of bottled
 207 tris 0.0007 higher than bagged tris (8.26327 \pm 0.0004, n = 6). The differences in filling procedure or impurities between
 208 bags and bottles in test 3 appear to have little effect on the initial pH. The mean initial pH of tris batch 4 is 0.002 (n =
 209 5) lower than calculated pH_{tris,20°C} (Fig. A2). This difference between the mean initial pH of tris batch 4 and calculated
 210 pH_{tris,20°C} is similar in direction and magnitude to those reported in other studies: DeGrandpre et al. (2014) reported –
 211 0.0012 \pm 0.0025 and Müller and Rehder (2018) reported -0.002 to -0.008 (measured pH minus pH_{tris,T_C}). With standard
 212 laboratory equipment and off-the-shelf reagents, an uncertainty of 0.006 is expected in prepared tris (Paulsen and
 213 Dickson, 2020). Measurements were also made on Dickson standard tris (batch T35) using the same instrument and
 214 the pH was 0.0019 higher than the calculated pH_{tris,20°C} (n = 2). In tests 1 and 2, the initial pH was extrapolated from
 215 a linear regression. The extrapolated initial pH values are more variable and lower (on average) than those directly

216 measured (Fig. A2). These differences may be a result of the extrapolation or different experimental variables such as
217 the increased rinsing of bags, or the single bag type and storage location used in test 3.

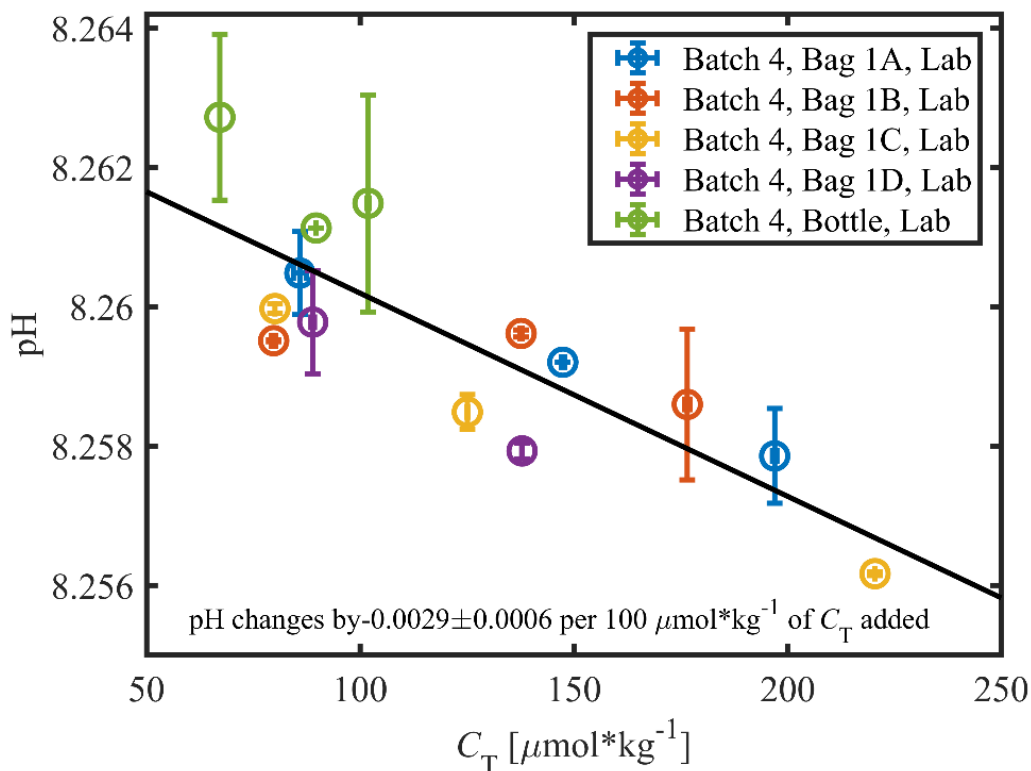


218
219 **Figure 3: Combined time series of measured pH in tris buffer tris buffer solutions. The dots represent every**
220 **measurement made on a (non-damaged) bag of tris. The dotted line is the “All Bags, All Batches, Lab or Tank”**
221 **regression. The grey shaded region is the observational 95% confidence interval (CI). The CI is intended to**
222 **estimate the future pH of a tris bag (with known initial pH and an unmeasured bag specific rate of change).**
223 **The upper and lower bounds are -0.0042 and -0.0076 pH per year, respectively.**

224 Figure 3 depicts a composite of all test results as the change from the initial pH of tris
225 ($\Delta pH = pH_{spec,20^\circ C}^{t=day} - pH_{spec,20^\circ C}^{t=0}$) as a function of time elapsed since bagging. A linear regression on all pH
226 measurements, excluding the outlier of “Batch 2, Bag 1, Lab”, of tris stored in bag types 1 or 2, has a slope of -0.0058
227 $\pm 0.0011 \text{ yr}^{-1}$ (mean \pm 95% C.I.). The upper and lower bounds of ΔpH at $t = 365$ days, -0.0042 and -0.0076 , are
228 important to consider when utilizing this bagged storage method of tris. These bounds provide the broadest expected
229 range in pH change over a year of storage, and include both the intercept and slope confidence intervals. The outlier
230 (Batch 2, Bag 1, Lab) was excluded due to noticeable damage to the bag (see Fig. A3 in Appendix A), which is
231 believed to have caused its pH to decrease at more than two times the average rate of the other bags. The damage
232 appears to be a break in the metallic bag layer, potentially caused by creasing or pinching of the bag when handling.
233 This observation highlights the importance of maintaining bag integrity, particularly during use in the field. A
234 successful two-week field deployment has been conducted using the tris bags described here and a modified SeapHOx
235 in a shallow, coral reef flat (Bresnahan et al. 2021). This two-week deployment was significantly shorter than the year
236 of storage described here and further field testing in longer deployments in varied environments are required before
237 widespread use of this technology. For the longer time frame depicted in Figure 3, the only comparable example found
238 in the literature is the work of Lai et al. (2018). In this work, Lai et al. (2018) used bagged tris for sensor calibration,
239 with in situ tris measurements made over 150 days. Lai et al. (2018) did not report a change in the pH of bagged tris

240 over the deployment; however, the reported precision of the SAMI-pH in situ instrument (± 0.003) would not resolve
241 the expected change shown in our Figure 3. Therefore, the results of Lai et al. (2018) are not inconsistent with our
242 study.

243 A significant increase in C_T was observed for all types of bags and bottles in Experiment 3 (Figure 4). A high
244 correlation between solution pH and C_T was observed, with a slope of -0.0029 ± 0.0006 pH per $100 \mu\text{mol kg}^{-1}$ ($n =$
245 $14, r^2 = 0.70$), suggesting that the change in tris pH and C_T was primarily driven by an increase in CO_2 . The observed
246 slope agrees closely with a theoretical model prediction of a linear decrease in pH of -0.0024 per $100 \mu\text{mol kg}^{-1}$ of
247 C_T added (over the range of C_T observed). There are two possible sources of the increasing C_T : gas exchange of CO_2
248 with the environment and microbial respiration within the storage vessel. Gas exchange should not be a significant
249 source of CO_2 for tris stored in a borosilicate bottle, as this is the standard equipment used to store seawater CO_2 and
250 tris buffers and is known to minimize gas exchange (Dickson et al. 2007). Therefore, it is likely that respiration was
251 the primary driver for the increase in C_T for tris stored in bottles. On average, pH decrease of tris stored in bags was
252 larger than that in the standard bottle (Figure 2), indicating either an additional source of CO_2 from gas exchange, or
253 larger amounts of respiration. Distinguishing between these two theorized sources would require measurements of
254 additional parameters such as dissolved organic carbon.



255
256 **Figure 4: pH plotted against C_T shows a linear relationship between the two parameters in tris buffer with a slope of $-$**
257 **0.0029 pH for every $100 \mu\text{mol kg}^{-1}$ of C_T added. The measurements shown are from three sampling occurrences between**
258 **130–300 days stored on bags and bottles used in Test 3. Only two measurements are shown for “Batch 4, Bag 1D, Lab”**
259 **because it ran empty before C_T were made.**

260 The pH stability of tris could be improved by reducing either likely source of C_T : gas exchange or microbial
261 respiration. For bags, CO_2 may diffuse through the fittings, gasket, or bag walls, particularly if damaged. The relatively
262 small breaks in the aluminium foil layer caused “Batch 2, Bag 1, Lab” to decrease more than twice as fast as the
263 average bag. Storage bag, fitting, and gasket material, as well as careful handling, are therefore important factors in
264 minimizing gas exchange. For example, silicone is permeable to CO_2 , and thus could have been a path of gas exchange
265 into the tris for this experiment. As noted above, Nemzer and Dickson (2005) found an almost negligible change of
266 0.5 mpH yr^{-1} in bottled tris. Our bottled tris changed at -3.0 mpH yr^{-1} ($n = 10$ bottles measured over 161 days),
267 approximately half the rate of the tris stored in bags. While -3.0 mpH yr^{-1} is near the detection limit of our
268 measurements, it suggests that the bottling protocol used in this study was not as well controlled as that of Nemzer
269 and Dickson (2005). For example, the Dickson lab at Scripps Institution of Oceanography regularly uses an annealing
270 oven to combust all trace organic films that may persist on glass bottles, but in our study, bottles were not annealed.
271 Although bags cannot be annealed, future steps that may be worth consideration to reduce microbial respiration in
272 bags include addition of a biocide to the tris solution, acid cleaning the bags, and using ultraviolet light to remove
273 organics from the ultrapure water used to prepare tris. There are some disadvantages to these proposed steps. Addition
274 of a biocide may not be ideal for use in sensitive environments if the tris is discharged after use and would alter the
275 composition of the solution slightly. While rinsing or prolonged soaking of the bags with an acid may help to remove
276 organics, it is unclear if it would have negative effects on the integrity of the bags. Beyond removing organics on the
277 bag surfaces, care should be taken to avoid introducing organic contaminants into the tris during the solution
278 preparation and bag filling procedures to minimize future respiration.

279 Both bag type 1 and 2 experienced problems with structural integrity during this experiment. A single type 2
280 bag experienced delamination of exterior bag layers when stored submerged in seawater, causing the eventual tearing
281 and failure of the bag when handling. Bag type 2 was not used in test 3 due to this failure. It should be noted that in
282 other studies which successfully used bag type 2, the bag was submerged in seawater for less time than in this
283 experiment (Sayles and Eck, 2009; Abmann et al., 2011; Wang et al., 2015). A single bag type 1 had the subtler
284 problem of small breaks in the aluminium foil bag layer, likely causing an increased pH rate of change. In non-
285 damaged bags, factors such as bag type/bottle, lab/tank storage, or tris batch did not have statistically significant (p -
286 value < 0.05) correlations with the pH change of tris (p -values 0.12, 0.11 and 0.09, respectively). The results of the
287 ANOVA support that tris can be held in bag type 1 or 2 and stored in a lab or tank and the pH will change similarly
288 regardless of storage method for up to 300 days. Additional bag types could be tested, such as bags made by Pollution
289 Measurement Corp. used by Lai et al. (2018) or Scholle DuraShield used by Takeshita et al. (2015).

290 These results suggest that when bags are carefully handled prior to and after filling, tris pH changes are small
291 over time. Specific recommendations for further work include: bags must be handled with care and enclosed in
292 protective containers to prevent damage, bags must be rinsed with tris prior to filling, and additional testing is merited
293 to determine sources of and methods to reduce contamination, such as acid washing.

294 **4. Conclusions**

295 This article describes our characterization of the stability of tris buffer in artificial seawater when stored in
296 purportedly gas-impermeable bags. Several different tests, initiated over the course of a year and a half and lasting up
297 to 300 days, exhibited an average decrease of 5.8 mpH yr⁻¹. In comparison, tris stored in standard borosilicate bottles
298 was shown to have a decrease of 3.0 mpH yr⁻¹. For yearlong deployments, an expected pH change of -0.0058 is well
299 below the weather quality threshold of 0.02 pH units. This low rate of change demonstrates the value of bagged tris
300 for in situ validation of autonomous pH sensors (regardless of sensor operating principles), particularly in highly
301 dynamic areas where repeatability of calibration based on discrete samples is challenging. Given the thorough
302 characterization of tris over wide ranges of environmental variables, this contribution can aid in the traceability and
303 intercomparability of pH sensor measurements. While valuable at the current stage of development (as demonstrated
304 by, e.g., Lai et al. (2018) and Bresnahan et al. (2021)), further development would ideally result in a commercially
305 available bag and filling procedure that can yield a rate of pH change less than the climate threshold of 0.003 per year.
306 This will require further tests to identify the source of CO₂, gas exchange or microbial respiration, as well as steps to
307 reduce or eliminate these sources.

308 Periodic measurement of bagged tris in situ would allow for detection of sensor drift. Most in situ pH sensors
309 are deployed in the euphotic zone in coastal areas, typically resulting in expedited biofouling and sedimentation, and
310 leading to sensor drift (Bresnahan et al., 2014) that could be identified and potentially corrected. Such periodic
311 calibration/validation would aid in identifying sensor issues and allow for greater consistency and continuity between
312 a timeseries and planned or vicarious crossovers where an automated calibration can be used to augment or replace
313 pre- and post-deployment calibrations/validations.

314 **Appendix A**

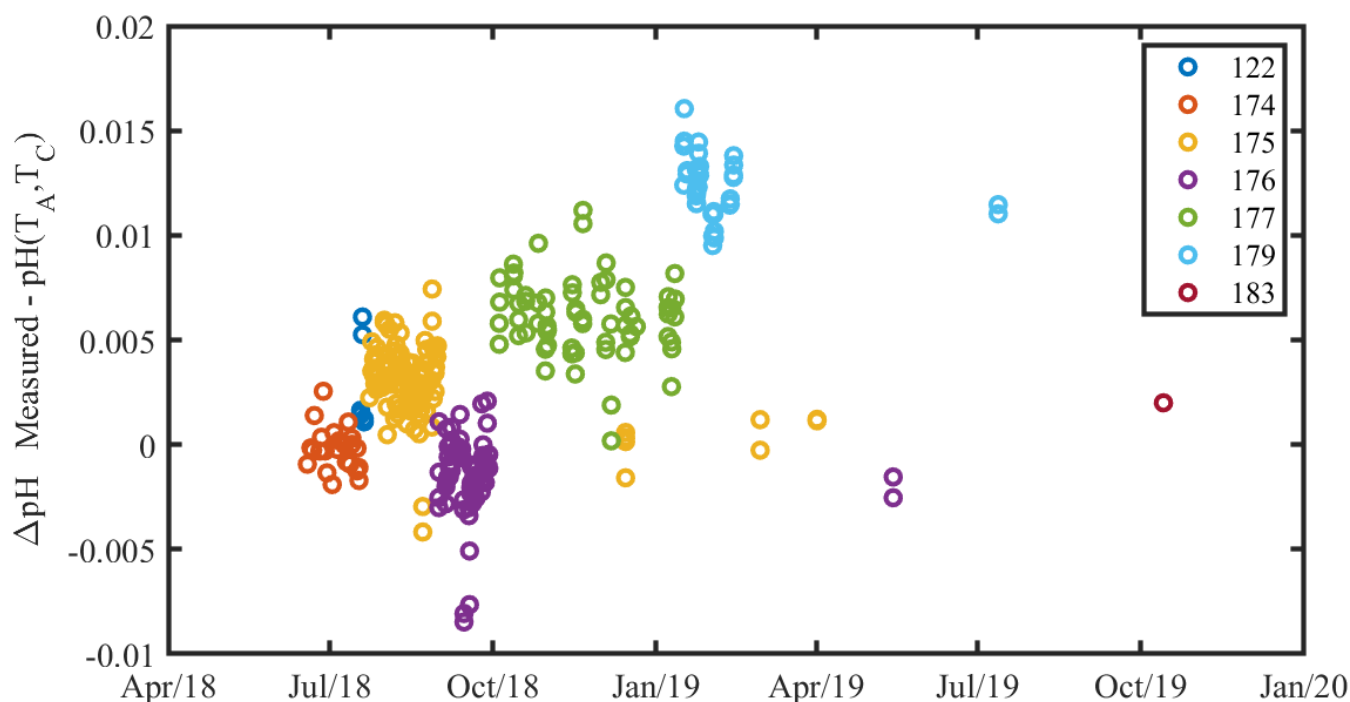
315

316 **Table A1. Detailed information about the specific reagents used to make the tris solution. *Reagent chemicals that meet or**
 317 **surpass specifications of the British Pharmacopeia (BP), European Pharmacopeia (EP), Food Chemicals Codex (FCC),**
 318 **United States Pharmacopeia (USP).**

319

| Chemical | Manufacture | Part Number | Lot Number | Batch | Assay | Grade |
|---------------------------------|-------------------|-------------|--------------|---------|----------------|----------------|
| tris | Fisher Scientific | T395-1 | 170360 | all | 99.8% | Certified ACS |
| NaCl | Fisher Scientific | S641-212 | 127252 | all | 99.0 to 100.5% | *BP/EP/FCC/USP |
| Na ₂ SO ₄ | Fisher Scientific | S421-1 | 134837 | all | 99.8% | Certified ACS |
| KCl | Fisher Scientific | P217-500 | 174416 | all | 99.7% | Certified ACS |
| MgCl ₂ | Teknova | M0304 | M030427E1401 | all | 1 M | Biotechnology |
| CaCl ₂ | Amresco | E506-500mL | 0982C098 | all | 0.95-1.05 M | Biotechnology |
| HCl | Fisher Scientific | SA48-1 | 175004 | 1, 2, 3 | 0.999 N | Certified |
| HCl | Fisher Scientific | SA48-1 | 188768 | 4 | 1.003 N | Certified |

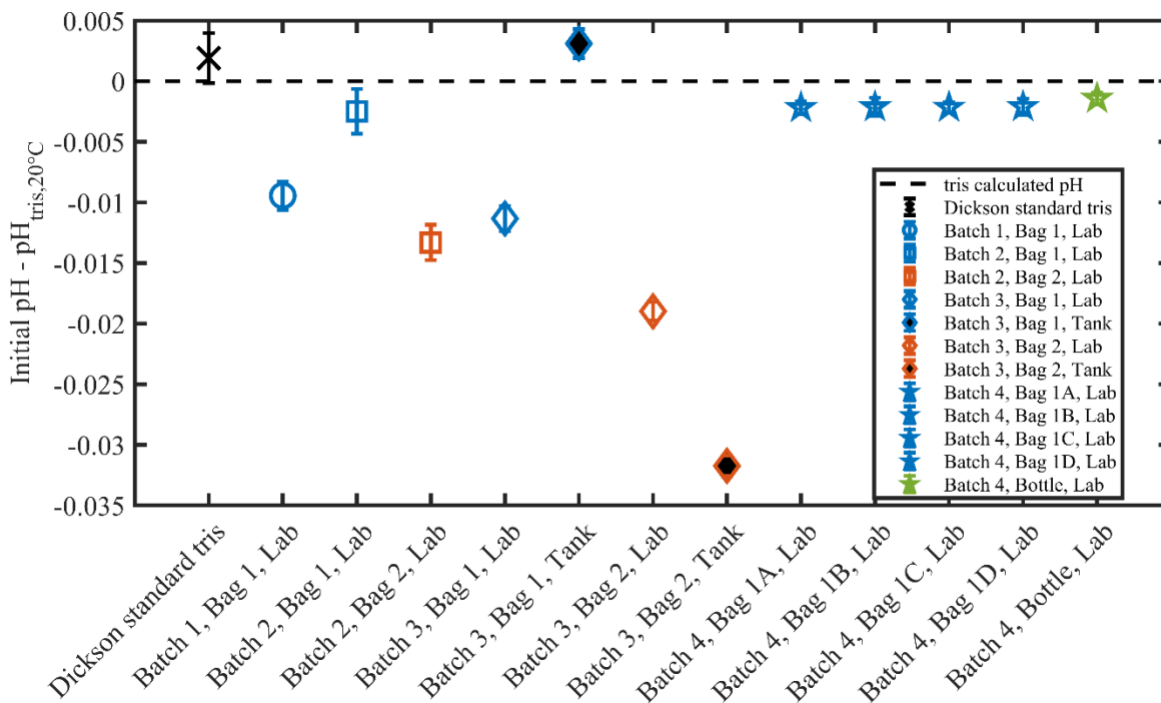
320



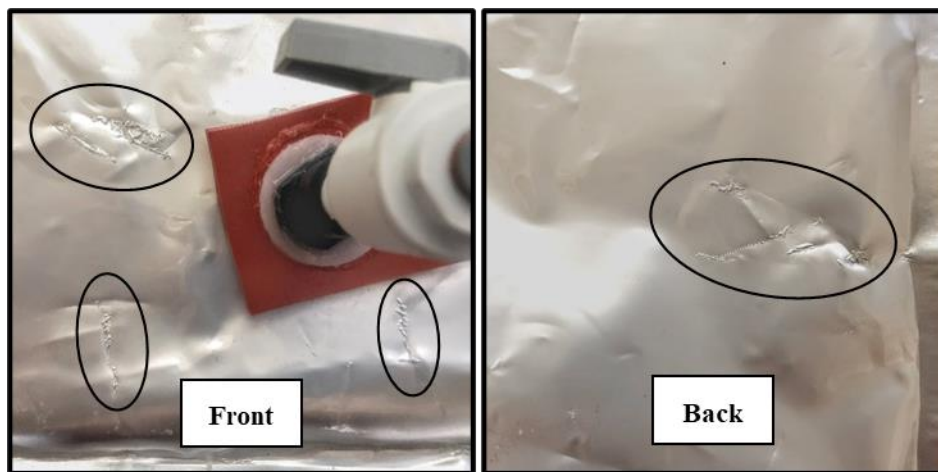
321

322 **Fig. A1: A timeseries of the residual between measured and calculated CRM pH throughout the experiment. Marker color**
 323 **denotes CRM batch number. There is a clear variability between measured and calculated pH, which typical of CRM**
 324 **batches (Andrew Dickson, *pers. comm.*). There was no observable systematic drift in the pH system during the experiment.**
 325 **The mean standard deviation of pH measurements within a CRM batch is 0.0016, which is comparable to the 0.0019**
 326 **reported in Bockmon & Dickson (2015). The same 760 nm absorbance wavelength outlier removal procedure used for tris**
 327 **measurements was applied to CRM measurements.**

328



329
 330 Fig. A2: The initial pH residual of each tris bag or bottle measured in this experiment. The initial pH is reported as a
 331 residual from the calculated pH at 20 °C. The initial pH was measured directly for tris batch 4 and extrapolated for
 332 tris batches 1-3. Additionally, 2 bottles of Dickson standard tris (show by the black “X”) were measured on
 333 12/10/2018. The zero black dashed line is the calculated pH of tris at 20 °C, based upon the measured reagent
 334 concentrations (DeValls and Dickson, 1998).



335
 336 Fig. A3. The ovals indicate marks on the exterior of “Batch 2, Bag 1, Lab”. These marks appear to be damage to the interior
 337 metallic layer, possibly due to creasing of the bag. These marks were not present on any other bag used in this study.

338
 339

340 **Author contribution**

341 WW performed formal analysis, visualization, and writing – original draft preparation. KS and TW contributed
342 to investigation and writing – review & editing. PB, YT, and TM contributed to funding acquisition, conceptualization,
343 formal analysis, and writing – review & editing.

344 **Competing interests**

345 The authors declare that they have no conflict of interest.

346 **Data availability**

347 pH and C_T data are available via the UC San Diego Library Digital Collections at
348 <https://doi.org/10.6075/J0QC022G> (Wolfe et al., 2021).

349 **Acknowledgements**

350 We thank May-Linn Paulsen and Andrew Dickson’s laboratory for sharing their tris expertise throughout this
351 project. We thank the National Science Foundation Ocean Technology and Interdisciplinary Coordination (NSF-OTIC
352 1736905 and NSF-OTIC 1736864) and the David and Lucile Packard Foundation for supporting this work.

353 **References**

- 354 ACT: Protocols for the Performance Verification of In Situ pH Sensors, Alliance for Coastal Technologies,
355 <https://doi.org/10.25607/OBP-331>, 2012.
- 356 Aßmann, S., Frank, C., and Kortzinger, A.: Spectrophotometric high-precision seawater pH determination for use in
357 underway measuring systems, *Ocean Sci.*, 7, 597-607, <https://doi.org/10.5194/os-7-597-2011>, 2011.
- 358 Bandstra, L., Hales, B., and Takahashi, T.: High-frequency measurements of total CO₂: Method development and first
359 oceanographic observations, *Mar. Chem.*, 100, 24-38, <https://doi.org/10.1016/j.marchem.2005.10.009>, 2006.
- 360 Bates, N., Astor, Y., Church, M., Currie, K., Dore, J., Gonzalez-Davila, M., Lorenzoni, L., Muller-Karger, F.,
361 Olafsson, J., and Santana-Casiano, J.: A Time-Series View of Changing Surface Ocean Chemistry Due to
362 Ocean Uptake of Anthropogenic CO₂ and Ocean Acidification, *J. Oceanogr.*, 27, 126-141,
363 <https://doi.org/10.5670/oceanog.2014.16>, 2014.
- 364 Bittig, H. C., Steinhoff, T., Claustre, H., Fiedler, B., Williams, N. L., Sauzède, R., Kortzinger, A., and Gattuso, J.-P.:
365 An Alternative to Static Climatologies: Robust Estimation of Open Ocean CO₂ Variables and Nutrient
366 Concentrations From T, S, and O₂ Data Using Bayesian Neural Networks, *Front. Mar. Sci.*, 5,
367 <https://doi.org/10.3389/fmars.2018.00328>, 2018.
- 368 Bockmon, E. E., and Dickson, A. G.: An inter-laboratory comparison assessing the quality of seawater carbon dioxide
369 measurements, *Mar. Chem.*, 171, 36-43, <https://doi.org/10.1016/j.marchem.2015.02.002>, 2015.
- 370 Branch, T. A., DeJoseph, B. M., Ray, L. J., and Wagner, C. A.: Impacts of ocean acidification on marine seafood,
371 *Trends Ecol. Evol.*, 28, 178-186, <https://doi.org/10.1016/j.tree.2012.10.001>, 2013.
- 372 Bresnahan, P. J., Takeshita, Y., Wirth, T., Martz, T. R., Cyronak, T., Albright, R., Wolfe, K., Warren, J. K., and Mertz,
373 K.: Autonomous in situ calibration of ion-sensitive field effect transistor pH sensors, *Limnology and
374 Oceanography: Methods*, 19, 132-144, <https://doi.org/10.1002/lom3.10410>, 2021.
- 375 Bresnahan, P. J., Martz, T. R., Takeshita, Y., Johnson, K. S., and LaShomb, M.: Best practices for autonomous
376 measurement of seawater pH with the Honeywell Durafet, *Methods Oceanogr.*, 9, 44-60,
377 <https://doi.org/10.1016/j.mio.2014.08.003>, 2014.

378 Bushinsky, S. M., Takeshita, Y., and Williams, N. L.: Observing changes in ocean carbonate chemistry: our
379 autonomous future, *Curr. Clim.*, 5, 207-220, <https://doi.org/10.1007/s40641-019-00129-8>, 2019.

380 Byrne, R. H.: Measuring Ocean Acidification: New Technology for a New Era of Ocean Chemistry, *Environ. Sci.*
381 *Technol.*, 48, 5352-5360, <https://doi.org/10.1021/es405819p>, 2014.

382 Carter, B., Radich, J., Doyle, H., and Dickson, A.: An automated system for spectrophotometric seawater pH
383 measurements, *Limnol. Oceanogr. Methods*, 11, 16-27, <https://doi.org/10.4319/lom.2013.11.16>, 2013.

384 Carter, B. R., Feely, R. A., Williams, N. L., Dickson, A. G., Fong, M. B., and Takeshita, Y.: Updated methods for
385 global locally interpolated estimation of alkalinity, pH, and nitrate, *Limnol. Oceanogr. Methods*, 16, 119-
386 131, <https://doi.org/10.1002/lom3.10232>, 2018.

387 Chavez, F., Pennington, J. T., Michisaki, R., Blum, M., Chavez, G., Friederich, J., Jones, B., Herlien, R., Kieft, B.,
388 Hobson, B., Ren, A., Ryan, J., Sevadjian, J., Wahl, C., Walz, K., Yamahara, K., Friederich, G., and Messié,
389 M.: Climate Variability and Change: Response of a Coastal Ocean Ecosystem, *J. Oceanogr.*, 30, 128-145,
390 <https://doi.org/10.5670/oceanog.2017.429>, 2017.

391 Cooley, S. R., and Doney, S. C.: Anticipating ocean acidification's economic consequences for commercial fisheries,
392 *Environ. Res. Lett.*, 4, 8, <https://doi.org/10.1088/1748-9326/4/2/024007>, 2009.

393 DeGrandpre, M. D., Spaulding, R. S., Newton, J. O., Jaqueth, E. J., Hamblock, S. E., Umansky, A. A., and Harris, K.
394 E.: Considerations for the measurement of spectrophotometric pH for ocean acidification and other studies,
395 *Limnol. Oceanogr. Methods*, 12, 830-839, <https://doi.org/10.4319/lom.2014.12.830>, 2014.

396 DelValls, T., and Dickson, A.: The pH of buffers based on 2-amino-2-hydroxymethyl-1,3-propanediol ('tris') in
397 synthetic sea water, *Deep Sea Res. Part I*, 45, 1541-1554, [https://doi.org/10.1016/S0967-0637\(98\)00019-3](https://doi.org/10.1016/S0967-0637(98)00019-3),
398 1998.

399 Dickson, A. G.: pH buffers for sea-water media based on the total hydrogen-ion concentration scale, *Deep Sea Res.*
400 *Part I*, 40, 107-118, [https://doi.org/10.1016/0967-0637\(93\)90055-8](https://doi.org/10.1016/0967-0637(93)90055-8), 1993.

401 Dickson, A. G.: Reference materials for oceanic CO₂ measurements, *J. Oceanogr.*, 14, 21-22, 2001.

402 Dickson, A. G., Sabine, C. L., and Christian, J. R.: Guide to Best Practices for Ocean CO₂ Measurements, PICES
403 Special Publication 3, North Pacific Marine Science Organization, Sidney, British Columbia, 191 pp., 2007.

404 Doney, S. C., Fabry, V. J., Feely, R. A., and Kleypas, J. A.: Ocean acidification: the other CO₂ problem, *Annu. Rev.*
405 *Mar. Science*, 1, 169-192, <https://doi.org/10.1146/annurev.marine.010908.163834>, 2009.

406 Doney, S. C., Busch, D. S., Cooley, S. R., and Kroeker, K. J.: The impacts of ocean acidification on marine ecosystems
407 and reliant human communities, *Annu. Rev. Environ. Resour.*, 45, <https://doi.org/10.1146/annurev-environ-012320-083019>, 2020.

409 Friederich, G., Walz, P., Burczynski, M., and Chavez, F.: Inorganic carbon in the central California upwelling system
410 during the 1997–1999 El Niño–La Niña event, *Prog. Oceanogr.*, 54, 185-203, [https://doi.org/10.1016/S0079-6611\(02\)00049-6](https://doi.org/10.1016/S0079-6611(02)00049-6), 2002.

412 Hales, B., Takahashi, T., and Bandstra, L.: Atmospheric CO₂ uptake by a coastal upwelling system, *Global*
413 *Biogeochem. Cycles*, 19, <https://doi.org/10.1029/2004gb002295>, 2005.

414 Johnson, K. S., Jannasch, H. W., Coletti, L. J., Elrod, V. A., Martz, T. R., Takeshita, Y., Carlson, R. J., and Connery,
415 J. G.: Deep-Sea DuraFET: A Pressure Tolerant pH Sensor Designed for Global Sensor Networks, *Anal.*
416 *Chem.*, 88, 3249-3256, <https://doi.org/10.1021/acs.analchem.5b04653>, 2016.

417 Johnson, K. S., Plant, J. N., Coletti, L. J., Jannasch, H. W., Sakamoto, C. M., Riser, S. C., Swift, D. D., Williams, N.
418 L., Boss, E., Haëntjens, N., Talley, L. D., and Sarmiento, J. L.: Biogeochemical sensor performance in the
419 SOCCOM profiling float array, *J. Geophys. Res.: Oceans*, 122, 6416-6436,
420 <https://doi.org/10.1002/2017jc012838>, 2017.

421 Karl, D. M.: Oceanic ecosystem time-series programs: Ten lessons learned, *J. Oceanogr.*, 23, 104-125,
422 <https://doi.org/10.5670/oceanog.2010.27>, 2010.

423 Lai, C.-Z., DeGrandpre, M. D., and Darlington, R. C.: Autonomous Optofluidic Chemical Analyzers for Marine
424 Applications: Insights from the Submersible Autonomous Moored Instruments (SAMI) for pH and pCO₂,
425 *Front. Mar. Sci.*, 4, <https://doi.org/10.3389/fmars.2017.00438>, 2018.

426 Liu, X. W., Patsavas, M. C., and Byrne, R. H.: Purification and Characterization of meta-Cresol Purple for
427 Spectrophotometric Seawater pH Measurements, *Environ. Sci. Technol.*, 45, 4862-4868,
428 <https://doi.org/10.1021/es200665d>, 2011.

429 Martz, T. R., Daly, K. L., Byrne, R. H., Stillman, J. H., and Turk, D.: Technology for ocean acidification research
430 needs and availability, *J. Oceanogr.*, 28, 40-47, <https://doi.org/10.5670/oceanog.2015.30>, 2015.

431 McLaughlin, K., Dickson, A., Weisberg, S. B., Coale, K., Elrod, V., Hunter, C., Johnson, K. S., Kram, S., Kudela, R.,
432 Martz, T., Negrey, K., Passow, U., Shaughnessy, F., Smith, J. E., Tadesse, D., Washburn, L., and Weis, K.

433 R.: An evaluation of ISFET sensors for coastal pH monitoring applications, *Reg. Stud. Mar. Sci.*, 12, 11-18,
434 <https://doi.org/10.1016/j.rsma.2017.02.008>, 2017.

435 Müller, J., Bastkowski, F., Sander, B., Seitz, S., Turner, D., Dickson, A., and Rehder, G.: Metrology for pH
436 Measurements in Brackish Waters-Part 1: Extending Electrochemical pH(T) Measurements of TRIS Buffers
437 to Salinities 5-20, *Front. Mar. Sci.*, 5, <https://doi.org/10.3389/fmars.2018.00176>, 2018.

438 Müller, J. D., and Rehder, G.: Metrology of pH Measurements in Brackish Waters—Part 2: Experimental
439 Characterization of Purified meta-Cresol Purple for Spectrophotometric pHT Measurements, *Front. Mar.
440 Sci.*, 5, 177, <https://doi.org/10.3389/fmars.2018.00177>, 2018.

441 Nemzer, B., and Dickson, A.: The stability and reproducibility of Tris buffers in synthetic seawater, *Mar. Chem.*, 96,
442 237-242, <https://doi.org/10.1016/j.marchem.2005.01.004>, 2005.

443

444 Newton, J., Feely, R., Jewett, E., Williamson, P., and Mathis, J.: *Global Ocean Acidification Observing Network:
445 Requirements and Governance Plan. Second Edition*, 2015.

446 O'Sullivan, D. W., and Millero, F. J.: Continual measurement of the total inorganic carbon in surface seawater, *Mar.
447 Chem.*, 60, 75-83, [https://doi.org/10.1016/s0304-4203\(97\)00079-0](https://doi.org/10.1016/s0304-4203(97)00079-0), 1998.

448 Okazaki, R. R., Sutton, A. J., Feely, R. A., Dickson, A. G., Alin, S. R., Sabine, C. L., Bunje, P. M. E., and Virmani,
449 J. I.: Evaluation of marine pH sensors under controlled and natural conditions for the Wendy Schmidt Ocean
450 Health XPRIZE, *Limnol. Oceanogr. Methods*, 15, 586-600, <https://doi.org/10.1002/lom3.10189>, 2017.

451 Paulsen, M. L., and Dickson, A. G.: Preparation of 2-amino-2-hydroxymethyl-1, 3-propanediol (TRIS) pHT buffers
452 in synthetic seawater, *Limnol. Oceanogr. Methods*, 18, 504-515, <https://doi.org/10.1002/lom3.10383>, 2020.

453 Papadimitriou, S., Loucaides, S., Rérolle, V., Achterberg, E. P., Dickson, A. G., Mowlem, M., and Kennedy, H.: The
454 measurement of pH in saline and hypersaline media at sub-zero temperatures: Characterization of Tris
455 buffers, *Mar. Chem.*, 184, 11–20, <https://doi.org/10.1016/j.marchem.2016.06.002>, 2016.

456 Pierrot, D., Neill, C., Sullivan, K., Castle, R., Wanninkhof, R., Lüger, H., Johannessen, T., Olsen, A., Feely, R. A.,
457 and Cosca, C. E.: Recommendations for autonomous underway pCO₂ measuring systems and data-reduction
458 routines, *Deep Sea Res. Part II*, 56, 512-522, <https://doi.org/10.1016/j.dsr2.2008.12.005>, 2009.

459 Rodriguez, C., Huang, F., and Millero, F. J.: The partial molal volume and compressibility of Tris and Tris-HCl in
460 water and 0.725 m NaCl as a function of temperature, *Deep Sea Res. Part I*, 104, 41-51,
461 <https://doi.org/10.1016/j.dsr.2015.06.008>, 2015.

462 Sabine, C., Sutton, A., McCabe, K., Lawrence-Slavas, N., Alin, S., Feely, R., Jenkins, R., Maenner, S., Meinig, C.,
463 and Thomas, J.: Evaluation of a new carbon dioxide system for autonomous surface vehicles, *J. Atmos.
464 Oceanic Technol.*, 37, 1305-1317, <https://doi.org/10.1175/JTECH-D-20-0010.1>, 2020.

465 Sayles, F. L., and Eck, C.: An autonomous instrument for time series analysis of TCO₂ from oceanographic moorings,
466 *Deep Sea Res. Part I*, 56, 1590-1603, <https://doi.org/10.1016/j.dsr.2009.04.006>, 2009.

467 Seidel, M. P., DeGrandpre, M. D., and Dickson, A. G.: A sensor for in situ indicator-based measurements of seawater
468 pH, *Mar. Chem.*, 109, 18-28, <https://doi.org/10.1016/j.marchem.2007.11.013>, 2008.

469 Sloyan, B. M., Wanninkhof, R., Kramp, M., Johnson, G. C., Talley, L. D., Tanhua, T., McDonagh, E., Cusack, C.,
470 O'Rourke, E., McGovern, E., Katsumata, K., Diggs, S., Hummon, J., Ishii, M., Azetsu-Scott, K., Boss, E.,
471 Ansoorge, I., Perez, F. F., Mercier, H., Williams, M. J. M., Anderson, L., Lee, J. H., Murata, A., Kouketsu, S.,
472 Jeansson, E., Hoppema, M., and Campos, E.: The Global Ocean Ship-Based Hydrographic Investigations
473 Program (GO-SHIP): A Platform for Integrated Multidisciplinary Ocean Sci., *Front. Mar. Sci.*, 6,
474 <https://doi.org/10.3389/fmars.2019.00445>, 2019.

475 Spaulding, R. S., DeGrandpre, M. D., Beck, J. C., Hart, R. D., Peterson, B., De Carlo, E. H., Drupp, P. S., and Hammar,
476 T. R.: Autonomous in Situ Measurements of Seawater Alkalinity, *Environ. Sci. Technol.*, 48, 9573-9581,
477 <https://doi.org/10.1021/es501615x>, 2014.

478 Sutton, A. J., Feely, R. A., Maenner-Jones, S., Musielwicz, S., Osborne, J., Dietrich, C., Monacci, N., Cross, J., Bott,
479 R., and Kozyr, A.: Autonomous seawater pCO₂ and pH time series from 40 surface buoys and the emergence
480 of anthropogenic trends, *Earth Syst. Sci. Data*, 421, <https://doi.org/10.5194/essd-11-421-2019>, 2019.

481 Takeshita, Y., Frieder, C. A., Martz, T. R., Ballard, J. R., Feely, R. A., Kram, S., Nam, S., Navarro, M. O., Price, N.
482 N., and Smith, J. E.: Including high-frequency variability in coastal ocean acidification projections,
483 *Biogeosciences*, 12, 5853-5870, <https://doi.org/10.5194/bg-12-5853-2015>, 2015.

484 Takeshita, Y., McGillis, W., Briggs, E. M., Carter, A. L., Donham, E. M., Martz, T. R., Price, N. N., and Smith, J. E.:
485 Assessment of net community production and calcification of a coral reef using a boundary layer approach,
486 *J. Geophys. Res.: Oceans*, 121, 5655-5671, <https://doi.org/10.1002/2016JC011886>, 2016.

487 Takeshita, Y., Martz, T. R., Coletti, L. J., Dickson, A. G., Jannasch, H. W., and Johnson, K. S.: The effects of pressure
488 on pH of Tris buffer in synthetic seawater, *Mar. Chem.*, 188, 1-5, [10.1016/j.marchem.2016.11.002](https://doi.org/10.1016/j.marchem.2016.11.002), 2017.

489 Takeshita, Y., Johnson, K. S., Martz, T. R., Plant, J. N., and Sarmiento, J. L.: Assessment of Autonomous pH
490 Measurements for Determining Surface Seawater Partial Pressure of CO₂, *J. Geophys. Res.: Oceans*, 123,
491 4003-4013, <https://doi.org/10.1029/2017jc013387>, 2018.

492 Takeshita, Y., et al.: Consistency and stability of purified meta-cresol purple for spectrophotometric pH measurements
493 in seawater, *Mar. Chem.*, in review.

494 Tilbrook, B., Jewett, E. B., DeGrandpre, M. D., Hernandez-Ayon, J. M., Feely, R. A., Gledhill, D. K., Hansson, L.,
495 Isensee, K., Kurz, M. L., Newton, J. A., Siedlecki, S. A., Chai, F., Dupont, S., Graco, M., Calvo, E., Greeley,
496 D., Kapsenberg, L., Lebrech, M., Pelejero, C., Schoo, K. L., and Telszewski, M.: An Enhanced Ocean
497 Acidification Observing Network: From People to Technology to Data Synthesis and Information Exchange,
498 *Front. Mar. Sci.*, 6, 21, <https://doi.org/10.3389/fmars.2019.00337>, 2019.

499 Wang, Z. A., Sonnichsen, F. N., Bradley, A. M., Hoering, K. A., Lanagan, T. M., Chu, S. N., Hammar, T. R., and
500 Camilli, R.: In Situ Sensor Technology for Simultaneous Spectrophotometric Measurements of Seawater
501 Total Dissolved Inorganic Carbon and pH, *Environ. Sci. Technol.*, 49, 4441-4449,
502 <https://doi.org/10.1021/es504893n>, 2015.

503 Wang, Z. A., Moustahfid, H., Mueller, A. V., Michel, A. P. M., Mowlem, M., Glazer, B. T., Mooney, T. A., Michaels,
504 W., McQuillan, J. S., Robidart, J. C., Churchill, J., Sourisseau, M., Daniel, A., Schaap, A., Monk, S.,
505 Friedman, K., and Brehmer, P.: Advancing Observation of Ocean Biogeochemistry, Biology, and
506 Ecosystems With Cost-Effective in situ Sensing Technologies, *Front. Mar. Sci.*, 6, 22,
507 <https://doi.org/10.3389/fmars.2019.00519>, 2019.

508 Williams, N. L., Juranek, L. W., Johnson, K. S., Feely, R. A., Riser, S. C., Talley, L. D., Russell, J. L., Sarmiento, J.
509 L., and Wanninkhof, R.: Empirical algorithms to estimate water column pH in the Southern Ocean, *Geophys.
510 Res. Lett.*, 43, 3415-3422, <https://doi.org/10.1002/2016gl068539>, 2016.

511 Wolfe, W. H., Shipley, K. M., Bresnahan, P. J., Takeshita, Y., Wirth, T., Martz, T. R.: Data from: Technical note:
512 stability of tris pH buffer in artificial seawater stored in bags. UC San Diego Library Digital
513 Collections. <https://doi.org/10.6075/J0QC022G>, 2021.